Electronic States of SnS and SnS^+: A Configuration Interaction Study

Dipankar Giri and Kalyan Kumar Das*

Physical Chemistry Section, Department of Chemistry, Jadavpur University, Kolkata 700032, India

Received: March 12, 2005; In Final Form: May 27, 2005

Ab initio based multireference configuration interaction calculations are carried out for SnS and its monopositive ion using effective core potentials. Potential energy curves and spectroscopic constants of the low-lying states of SnS and SnS^+ are computed. The ground-state dissociation energies of the neutral and ionic species are about 4.71 and 2.86 eV, respectively which compare well with the available thermochemical data. The effect of d-electron correlation on the spectroscopic constants of a few low-lying states has been studied. The spin−orbit interaction has also been included to investigate its effect on the spectroscopic properties of both SnS and SnS^+. Dipole moment and transition moment curves are also constructed as a function of the bond length. Transition probabilities of some dipole-allowed and spin-forbidden transitions are studied. Radiative lifetimes of a few low-lying states are estimated. The $E^1\Sigma^+-X^1\Sigma^+$ transition of SnS is predicted to be the strongest one. The components of the $A^2\Sigma^+_{1/2}-X_2{}^2\Pi_{1/2}$ transition with parallel and perpendicular polarization are separately analyzed. The vertical ionization energies of the ground-state SnS to the ground and low-lying excited states of the monopositive ion are calculated.

I. Introduction

The oxides and sulfides of group IV are often used in chemical lasers. The electronic structure and spectroscopic properties of these molecules are the subject of many experimental and theoretical research for several years in the past.[1−26] The spectra of these molecules are comparable with those of CO which is well-known in the literature. In the mid-1930s of the 20th Century, several investigations[1−4] of the absorption and emission spectra of the diatomic tin sulfide molecule had been carried out. Douglas et al.[5] studied high-resolution absorption and emission spectra of SnS using the ^{120}Sn isotope. A simple $^1\Pi-^1\Sigma^+$ band system was found between 4000 and 3300 Å. The rotational and vibrational constants of the ground state of SnS are determined from these bands. Moreover, a band system, which lies between 3300 and 2500 Å, has been shown to be a $^1\Sigma^+-^1\Sigma^+$ system. Barrow et al.[6] have studied the absorption spectrum of SnS vapor in the ultraviolet and Schumann region. The spectroscopically determined dissociation energy (D^0_0) of SnS is 111 ± 6 kcal mol^{-1}. A much lower value D^0_0(SnS) ≤ 68.5 kcal mol^{-1} has been predicted on the basis of a supposed predissociation[3, 4] in the $A^1\Pi-X^1\Sigma^+$ system. A mass-spectrometric investigation of the vapor in equilibrium with solid SnS and PbS, and a mixture of SnS and PbS has been made by Collin and Drowart.[7] A value of D^0_0(SnS) = 110 ± 3.0 kcal mol^{-1} has been reported and compared with the spectroscopically determined value.[6]

Yamdagni and Joshi[8] have reinvestigated the visible absorption spectrum of SnS. Two systems such as B−X and C−X have been recognized. The absorption and fluorescence spectra of SnS and SnO have been studied in the 14000−50000 cm^{-1} region in inert gas matrixes[9] at 20 K. It showed one clear and sharp absorption due to the $D^1\Pi-X^1\Sigma^+$ system consisting of a progression of vibrational bands. The transition energy of the $D^1\Pi$ state of SnS has been reported to be 28360 cm^{-1}. The excitation of the D state for SnO and SnS has resulted a strong fluorescence which is attributed to the spin-forbidden $a^3\Pi-X^1\Sigma^+$ transition. The reported transition energy of the $a^3\Pi$ state of SnS is 18300 cm^{-1}. The infrared spectra of some matrix-isolated germanium, tin, and lead chalconides are reported[10] in argon and nitrogen matrices at 12 K. The electronic spectrum[11] of SnS, which is excited in chemiluminescence, has led to the characterization of two low-lying excited states such as $a\Omega1$-($^3\Sigma^+$) with T_e = 18143.9 cm^{-1} and $A0^+$($^3\Pi$) with T_e = 22021.3 cm^{-1}. The extended rotational analyses of the perturbed bands observed in the absorption spectrum enable the assignments of the $\Omega0^+$ and $\Omega1$ components of $^3\Sigma^-$, and $\Omega1$ of $^3\Pi$ for SnS. The observed T_e values of $C0^+$($^3\Sigma^-$) and $C'1$($^3\Sigma^-$) are 22380 and 22480 cm^{-1}, respectively, while that of $B\Omega1$($^3\Pi$) is about 23320 cm^{-1}. The observed spectrum has been found to be quite complex in character. As a result, the assignments of many observed progressions into the electronic band systems have been made with difficulties and uncertainties.

In general, theoretical studies of tin chalconides are limited in number. Ab initio based relativistic configuration interaction (CI) calculations of the low-lying electronic states of SnO and SnS are performed by Balasubramanian and co-workers.[12,13] Nair et al.[14] have calculated the potential energy curves and dissociation energies of the oxides and sulfides of group IVA elements for which sufficient spectroscopic data are available. Recently,[15] a MRDCI study has been made on the electronic spectrum of tin oxide. Dipole moments of the sulfides of Pb, Sb, and Sn have been calculated from the Stark effect measurements. Hoeft et al.[16,17] have reported the electric dipole moment of the ground-state ^{120}Sn^{32}S as 3.18 ± 0.10 D, while the value obtained by Narasimha and Curl[18] is about 3.38 ± 0.07 D. Nonrelativistic and relativistic high level correlated calculations have been carried out recently[19] for the determination of the dipole moments of the oxides and sulfides of lead and tin. Lafebvre et al.[20] have calculated the electronic structures of tin monochalconides (SnX; X = O, S, Se, and Te) using density functional pseudo-potential and tight binding theories.

Although the spectroscopy of the neutral oxides and sulfides of group IVA elements is well studied, the corresponding

* Corresponding author. E-mail: das_kalyank@yahoo.com or kkdas@chemistry.jdvu.ac.in.

10.1021/jp051290e CCC: $30.25
Published on Web 07/23/2005

monopositive ions are less known. The photoelectron spectra of the isovalent CO molecule are, however, well-known in the literature. A few decades ago, the vacuum UV photoelectron spectra of silicon and germanium monoxides have been recorded in the gas phase.[21−23] The He I photoelectron spectra of the ground state of the SnO molecule have been studied by Dyke et al.[24] These spectra are found to be very similar to those of CO. Two low-lying states such as $^2\Sigma^+$ and $^2\Pi$ of SnO^+ are characterized, and two bands are observed in the ionization energy range 9.5−11.0 eV because of heating SnO_2. The vibrational structure of the first band provides spectroscopic constants of the $X^2\Pi$ state of SnO^+. Recently,[25] four ionization energies of tin monoxide have been determined from the absorption spectrum in the range 2000−300 Å. However, the photoelectron spectrum of the ground-state SnS molecule is not yet known. Theoretical calculations of SnS^+ are also lacking. Ab initio based MRDCI calculations of the low-lying states of the isovalent SnO^+ have been carried out recently[26] using relativistic effective core potentials. The potential energy curves and spectroscopic parameters of the lowest few states are reported. Transition probabilities of different components of the A−X transition in the presence of the spin−orbit coupling are analyzed.

In this work we have performed ab initio based MRDCI calculations to study the structural and spectroscopic aspects of low-lying electronic states of SnS and SnS^+ including relativistic effects and the spin−orbit coupling. Some of the important transitions are investigated. The nature of the dipole moment and transition dipole moment functions for both neutral and ionic species is also the subject of the present study. The vertical ionization energies of the ground-state SnS are computed. The radiative lifetimes of some of the excited states are estimated.

II. Method of Computation

The relativistic effective core potentials (RECP) of both Sn and S atoms are used in the present calculations. For the heavier Sn atom, the RECP of LaJohn et al.[27] have been substituted for the core electrons, while $4d^{10}5s^25p^2$ electrons remain in the valence space. The RECP of Pacios and Christiansen[28] are used for the sulfur atom with the $3s^23p^4$ electrons in the valence space. The total numbers of active electrons to be treated in the CI calculations are 20 for SnS, and 19 for SnS^+. The starting primitive Gaussian basis functions[27] of Sn are (3s3p4d) without any contraction. These are compatible with the semicore RECP mentioned above. These basis functions of Sn are augmented with d and f polarization functions[29] ($\zeta_d = 0.08\ a_o^{-2}$ and $\zeta_f = 0.20\ a_o^{-2}$). A set of diffuse s function ($\zeta_s = 0.015\ a_o^{-2}$) and p functions ($\zeta_p = 0.012\ a_o^{-2}$) is added to make the final basis set of the type (4s4p5d1f) for the Sn atom. The (4s4p) Gaussian basis sets of the sulfur atom, taken from Pacios and Christiansen,[28] have been extended by adding two-member d-polarization functions of exponents 0.66 and 0.18 a_o^{-2} which are optimized by Lingott et al.[30] for the ^3P state of the sulfur atom at the CI level. A set of f functions with exponent 0.9 a_o^{-2}, optimized by these authors from the CI calculations of the ^1D excited state of S, has also been included in the basis. Therefore, the final basis set of S is of the type (4s4p2d1f).

The molecule and its ion are kept along the $+z$ axis with Sn at the origin. The computations are carried out in the C_{2v} symmetry. Using the above-mentioned ECP and basis sets, the self-consistent field (SCF) calculations are carried out for a particular low-lying state to generate optimized symmetry adapted molecular orbitals (MO). The SCF-MOs of the $(\pi^4\pi^{*2})^3\Sigma^-$ state of SnS and those of the $(\sigma\pi^4)^2\Sigma^+$ state of SnS^+ are used as one-electron basis orbitals for the generation of configurations in the CI calculations. It has been noted earlier that the $^3\Sigma^-$ and $^2\Sigma^+$ states of the isovalent SnO and SnO^+, respectively are suitable choices for the SCF-MO calculations as these will treat the π_x and π_y components in equal footing. The eigenvalues and eigenfunctions in the B_1 and B_2 representations are retained in their perfect symmetries so that there are no symmetry breaking solutions throughout the calculations. In the CI steps, the $4d^{10}$ electrons of Sn are found to be localized and they do not participate in the formation of low-lying electronic states of both SnS and SnS^+. Therefore, only 10 valence electrons for SnS and 9 for SnS^+ are allowed to excite for the construction of the configuration state functions. The MRDCI method of Buenker and co-workers[31−37] has been used throughout the calculations. The perturbative corrections and energy extrapolation techniques are employed here. For each spatial and spin symmetry, a set of reference configurations is chosen representing a particular low-lying state. The number of reference configurations varies depending upon the spatial and spin symmetry. Singlet, triplet, and quintet states of SnS and doublet and quartet states of SnS^+ are studied here. A maximum of eight roots in each symmetry is optimized. Within a chosen set of 100−200 reference configurations, the number of generated configurations arising out of all single and double excitations becomes as large as 10 million. However, with the choice of a configuration-selection threshold $T = 3.0\ \mu E_h$, the number of selected configurations reduces below 50000 for both the neutral and ionic species. The sums of the squares of the coefficients of reference configurations for the lowest few roots do not go below 0.90. Using the energy extrapolation method, one gets an estimate of energy at $T = 0$. The higher order excitations are taken into account by the multireference analogue of the Davidson correction.[38] The full-CI energies of the Λ−S states are thus estimated.

The effect of the spin−orbit coupling has been determined from a separate two-step variational calculations. In the spin-included Hamiltonian matrix, the diagonals are the full-CI energies of the Λ−S CI calculations, while the off-diagonals are computed from the RECP based spin−orbit operators and CI wave functions. The Wigner-Eckart theorem is employed to compute the spin−orbit matrix elements. The low-lying Ω-states belong to A_1, A_2, and B_1 representations for SnS, and to the degenerate E_1 and E_2 representations for SnS^+ in the C_{2v} double group. The spectroscopic constants are estimated from the potential curves. The radiative lifetime of a given vibrational level can then be computed from the Einstein spontaneous emission coefficients.

III. Spectroscopic Properties of Low-Lying Λ−S States

A. SnS. The ground states of both Sn and S atoms belong to the ^3P_g state. The interaction between these two states generates as many as 18 states of singlet, triplet, and quintet spin multiplicities. On the other hand, the first excited state (^1D_g) of Sn combines with the ground state of S to correlate with nine triplets. Table 1 shows the difference between the relative energies of the lowest two dissociation limits of SnS. The agreement between the computed data and the observed one from the atomic spectral study[39] is found to be good. The discrepancy is only within 100 cm^{-1}. Potential energy curves of all 18 Λ−S states dissociating into the lowest asymptote Sn(^3P_g) + S(^3P_g) are shown in Figure 1.

Spectroscopic constants of 13 states of Λ−S symmetries within 7 eV of energy are tabulated in Table 2. The ground

TABLE 1: Molecular States of SnS and Their Correlation with Atomic Limits

molecular state	atomic state Sn + S	relative energy/cm^{-1} exptl[a]	relative energy/cm^{-1} calcd
$^1\Sigma^+(2)$, $^1\Sigma^-$, $^1\Pi(2)$, $^1\Delta$, $^3\Sigma^+(2)$, $^3\Sigma^-$, $^3\Pi(2)$, $^3\Delta$, $^5\Sigma^+(2)$, $^5\Sigma^-$, $^5\Pi(2)$, $^5\Delta$	$^3P_g + {}^3P_g$	0	0
$^3\Sigma^+$, $^3\Sigma^-(2)$, $^3\Pi(3)$, $^3\Delta(2)$, $^3\Phi$	$^1D_g + {}^3P_g$	5764	5848

[a] Reference 39.

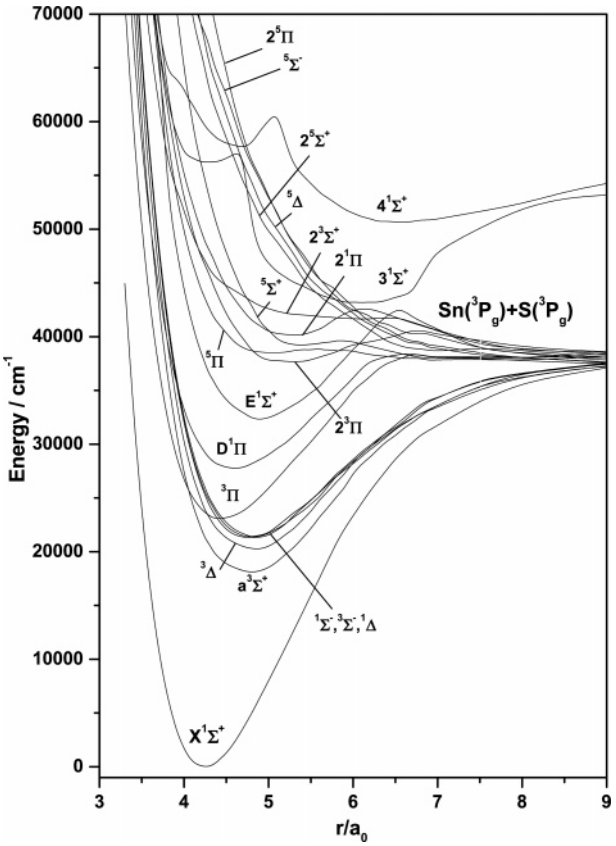

Figure 1. Potential energy curves of low-lying Λ−S states of SnS.

state of SnS is $X^1\Sigma^+$ comprising a dominant closed shell configuration, $\sigma^2\pi^4$. The MRDCI estimated bond length of the ground state is 2.25 Å, which is longer than the experimental one by about 0.04 Å. However, the present value is an improved one over the earlier calculated data. The inclusion of all $4d^{10}$ electrons in the CI calculations reduces the bond length by 0.01 Å. The computed ground-state vibrational frequency of 482 cm^{-1} agrees very well with the experimentally determined value of 487.26 cm^{-1}. The d-correlation does not change the frequency much. Thermochemical[6] dissociation energy of the ground-state SnS is reported to be about 4.77 eV, which also compares well with the calculated value of 4.71 eV without considering the spin−orbit coupling. However, the previous relativistic calculations[13] show a somewhat smaller D_e value of 4.2 eV.

The first excited state of SnS is of the $a^3\Sigma^+$ symmetry. In the chemiluminescence of SnS, an excited state, $a\Omega1(^3\Sigma^+)$ with $T_e = 18143.9$ cm^{-1} has been reported by Greenwood et al.[11] As seen in Table 2, the computed transition energy of the $a^3\Sigma^+$ state without spin−orbit coupling is about 18080 cm^{-1}, which compares well with the observed value. The $a^3\Sigma^+{}_1$ state has been detected only in the matrix spectra of the $a^3\Sigma^+{}_1-X^1\Sigma^+{}_{0^+}$ system in fluorescence.[9] The CI calculations involving all 10

TABLE 2: Spectroscopic Constants of Low-Lying Λ−S States of SnS

state	T_e/cm^{-1}	r_e/Å	ω_e/cm^{-1}
$X^1\Sigma^+$	0	2.25 (2.24)[a]	482 (483)[a]
		2.209[b]	487.26[b]
		2.32[c]	449[c]
$a^3\Sigma^+$	18080 (16360)[a]	2.53 (2.48)[a]	305 (312)[a]
	21864[c]	2.55[c]	356[c]
	18143.9[d]		
$^3\Delta$	20030 (19320)[a]	2.51 (2.59)[a]	327 (373)[a]
	24000[c]		
$^1\Sigma^-$	21190	2.52	322
	25685[c]	2.62[c]	307[c]
$^1\Delta$	21310 (20940)[a]	2.53 (2.53)[a]	318 (306)[a]
$c^3\Sigma^-$	21445	2.53	319
$b^3\Pi$	23120 (22160)[a]	2.35 (2.37)[a]	361 (345)[a]
	28658[c]	2.42[c]	377[c]
$D^1\Pi$	27720 (26780)[a]	2.43 (2.46)[a]	316 (341)[a]
	28336.6[b]	2.3569[b]	331.35[b]
	32707[c]	2.48[c]	371[c]
$E^1\Sigma^+$	32450 (31930)[a]	2.59 (2.50)[a]	287 (342)[a]
	33037.0[b]		294.25[b]
	41238[c]	2.63[c]	336[c]
$2^3\Pi$	37560	2.76	240
$2^1\Pi$	40130	2.80	238
$3^1\Pi$	50900	2.42	388
$3\ ^1\Sigma^+$	56220	2.26	311

[a] Numbers in parentheses refer to the 20-electron CI calculations. [b] Reference 9. [c] Reference 13. [d] Energy refers to the observed state, $a\Omega1(^3\Sigma^+)$.[11]

electrons of Sn in the 4d orbital produce a lower transition energy of 16360 cm^{-1}. The computed equilibrium bond length and vibrational frequency of the $a^3\Sigma^+$ state are 2.53 Å and 305 cm^{-1}, respectively. The d-correlation is shown to reduce the bond length of this state to 2.48 Å, while the ω_e value does not change much. The present spectroscopic parameters of this state are found to be improved over those of earlier calculations.[13] Like the oxide, the $a^3\Sigma^+$ state of SnS is characterized mainly by a singly excited $\pi \rightarrow \pi^*$ configuration. The state is strongly bound with a binding energy of about 2.47 eV as calculated from the MRDCI energies.

Five other states, namely, $^3\Delta$, $^1\Sigma^-$, $^1\Delta$, $c^3\Sigma^-$, and $E^1\Sigma^+$, which are dominated by the same $\pi^3\pi^*$ configuration as that in $a^3\Sigma^+$, are also bound. The calculations suggest that the $^3\Sigma^-$, $^1\Sigma^-$, and $^1\Delta$ states are nearly degenerate. The computed transition energies (T_e) of these states lie in the range 21100−21500 cm^{-1}. The $^3\Delta$ state is lying somewhat lower than these three states with a transition energy of 20030 cm^{-1}. The d-electron correlation reduces the transition energies of these states by about 350−750 cm^{-1}. The computed bond lengths of these states except $E^1\Sigma^+$ fall in the range 2.51−2.53 Å. Although $^3\Delta$, $^1\Sigma^-$, $^1\Delta$, and $c^3\Sigma^-$ states are not so important for transitions to the ground state, some of the spin components such as $^3\Delta_1$, $C^3\Sigma^-{}_{0^+}$, and $C'^3\Sigma^-{}_1$ may undergo weak spin-forbidden transitions to the ground-state component ($X^1\Sigma^+{}_{0^+}$). Specifically, the $^3\Sigma^-{}_{0^+,1}-X^1\Sigma^+{}_{0^+}$ transitions are expected to take place in the region 21000−22000 cm^{-1}. The $E^1\Sigma^+$ state is, however, less strongly bound with a MRDCI estimated binding energy of about 1.30 eV. This state is the second root of the $^1\Sigma^+$ symmetry. The computed T_e of the state is close to 32450 cm^{-1} as compared with the observed T_{00} of 33037 cm^{-1}.[13] The vibrational frequency computed here agrees well with the experimentally determined ω_e value. The potential minimum of the state is expected to be around 2.59 Å, which is 0.34 Å longer than that of the ground state. However, the 20-electron CI calculations reduce r_e of the $E^1\Sigma^+$ state by 0.09 Å. The potential energy curve shows that there is a small barrier near the bond length

TABLE 3: Molecular States of SnS^+ and Their Correlation with Atomic Limits

molecular state	atomic state $Sn^+ + S$	relative energy/cm^{-1} exptl[a]	relative energy/cm^{-1} calcd
$^2\Sigma^+$, $^2\Sigma^-(2)$, $^2\Pi(2)$, $^2\Delta$, $^4\Sigma^+$, $^4\Sigma^-(2)$, $^4\Pi(2)$, $^4\Delta$	$^2P_u + {}^3P_g$	0	0
$^2\Sigma^+(2)$, $^2\Sigma^-$, $^2\Pi(3)$, $^2\Delta(2)$, $^2\Phi$	$^2P_u + {}^1D_g$	9106.7	10257

[a] Reference 39.

of 3.45 Å (~6.5 a_o). As a result of the avoided crossing with the higher repulsive $3^1\Sigma^+$ state, the $E^1\Sigma^+$ state dissociates into the lowest limit $Sn(^3P_g) + S(^3P_g)$. In the Franck−Condon region, the $\pi^3\pi^*$ configuration interacts predominantly with a closed shell π^4 and a couple of excited configurations such as $\pi^2\pi^{*2}$ and $\sigma\sigma^*\pi$.[4] The $E^1\Sigma^+ - X^1\Sigma^+$ transition is expected to have a stronger intensity.

The $b^3\Pi$ state of SnS is located just above the set of nearly degenerate Σ^- and Δ states. The computed transition energy of the $b^3\Pi$ state at equilibrium is around 23120 cm^{-1} with r_e = 2.35 Å and ω_e = 361 cm^{-1}. The $b^3\Pi - X^1\Sigma^+$ spin-forbidden band is very similar to the Cameron band of CO. In fact, Greenwood et al.[11] have investigated several bands from the rotational analysis of the SnS molecule. The assignments of the $B1(^3\Pi) - X^1\Sigma^+$ and $A^3\Pi_{0^+} - X^1\Sigma^+$ systems have been made around 23320 and 22021 cm^{-1}, respectively. The CI wave functions of the $b^3\Pi$ state are characterized mainly by $\sigma\pi^4\pi^*$, and in the Franck−Condon region, it contributes more than 80%. As a result of the $\sigma \rightarrow \pi^*$ excitation, the Sn−S bond in the $b^3\Pi$ state is weaker than that in the ground state. In earlier calculations,[13] the spectroscopic parameters of this state are overestimated as compared in Table 2.

The same singly excited configuration dominates in the singlet counterpart of the $b^3\Pi$ state, and it is designated here as $D^1\Pi$. The compositions of these two states are quite similar. The $D^1\Pi - X^1\Sigma^+$ absorption system of SnS has been reported in the inert matrices with T_{00} = 28923 cm^{-1}. The same types of bands are known for other isovalent molecules such as GeO, SiO, SiS, SnO, etc. The computed transition energy (T_e) of the $D^1\Pi$ state of SnS is smaller than the observed value by about 600 cm^{-1}. The equilibrium bond length of this state is calculated to be longer than the experimentally determined value by 0.07 Å, while ω_e is smaller only by 15 cm^{-1}. Spectroscopically, the $D^1\Pi - X^1\Sigma^+$ transition is expected to be strong. The estimation of the radiative lifetime for such transition shows the quantitative feature which is discussed in the later section. A few more excited states of SnS are also reported in Table 2. The potential curves of higher Π states such as $2^3\Pi$ and $2^1\Pi$ are shallow. The third root of the $^1\Sigma^+$ symmetry undergoes an avoided crossing with a repulsive higher root near r = 2.5 Å. A very sharp minimum in the $3^1\Sigma^+$ curve is located in the energy region of 56220 cm^{-1} with a shorter bond length of 2.26 Å.

B. SnS^+. The monopositive tin and neutral sulfur both in their ground states correlate with the lowest dissociation limit of the SnS^+ ion. As shown in Table 3, there are six doublets and six quartets of Σ^+, $\Sigma^-(2)$, $\Pi(2)$, and Δ symmetries correlating with the $Sn^+(^2P_u) + S(^3P_g)$ limit. Another set of nine excited doublet states of SnS^+ correlates with the second dissociation limit $Sn^+(^2P_u) + S(^1D_g)$. The computed energy separation between the lowest two dissociation limits is larger than the value obtained from the atomic spectral energy levels[39] by about 1000 cm^{-1}. Figure 2 shows the potential energy curves of all 12 electronic states, which correlate with the lowest dissociation limit. Spectroscopic constants of seven $\Lambda - S$ states of SnS^+ are reported in Table 4. The ground-state symmetry of SnS^+ is $X^2\Pi$. The computed r_e and ω_e values of $X^2\Pi$ are 2.41 Å and 375 cm^{-1}, respectively. These constants do not change much when calculated with 19 electrons in the CI step. The ground-state bond of SnS^+ is about 0.35 Å longer than that of SnO^+. The first excited state, $A^2\Sigma^+$ is located only 3880 cm^{-1} above the ground state. However, 19-electron CI calculations reduce the gap by 545 cm^{-1}. The equilibrium bond length of SnS^+ in the $A^2\Sigma^+$ state is shorter by 0.15 Å, while the vibrational frequency at equilibrium is larger by about 60 cm^{-1} as compared to the ground-state parameters. The experimental photoelectron spectrum of SnS is not clearly known. The $A^2\Sigma^+ - X^2\Pi$ transition is expected to carry sufficient intensity. The quantitative aspect of this transition is discussed later on. The ground state of SnS^+ is dominated by the $\sigma^2\pi^3$ configuration, while the $\sigma \rightarrow \pi$ transition generates the $A^2\Sigma^+$ state. Three weakly bound quartets such as $^4\Pi$, $^4\Sigma^+$, and $^4\Delta$ are low-lying (see Figure 2). The computed transition energy of $^4\Pi$ is about 16060 cm^{-1} at r_e = 2.96 Å. The potential energy curve of $^4\Delta$ is very shallow with ω_e = 75 cm^{-1} only. However, none of these quartets is spectroscopically significant. The second root of the $^2\Pi$ symmetry has a very broad potential minimum around 18830 cm^{-1}.

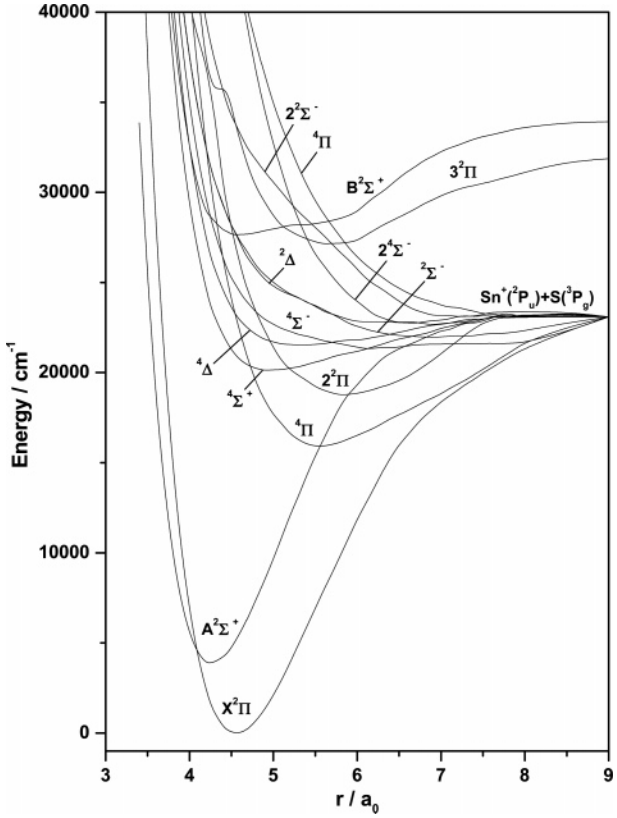

Figure 2. Potential energy curves of low-lying $\Lambda - S$ states of SnS^+.

TABLE 4: Spectroscopic Constants of Low-Lying $\Lambda - S$ States of SnS^+ [a]

state	T_e/cm^{-1}	r_e/Å	ω_e/cm^{-1}
$X^2\Pi$	0	2.41 (2.41)	375 (386)
$A^2\Sigma^+$	3880 (3335)	2.25 (2.26)	432 (423)
$^4\Pi$	16060	2.96	191
$2^2\Pi$	18830	3.10	178
$^4\Sigma^+$	20130 (19591)	2.63 (2.69)	175 (169)
$^4\Delta$	21480	2.91	75
$3^2\Pi$	27235	3.06	167
$B^2\Sigma^+$	27770	2.44	195

[a] Numbers in parentheses refer to 19-electron CI calculations.

TABLE 5: Spectroscopic Constants of Ω States of SnS

state	T_e/cm^{-1}	r_e/Å	ω_e/cm^{-1}	composition at r_e (% contribution)
$X^1\Sigma^+{}_{0^+}$	0	2.25	481	$X^1\Sigma^+$ (99)
$a^3\Sigma^+{}_1$	17710 (18143.9)[a]	2.53	306 (337.7)[a]	$a^3\Sigma^+$ (90), $c^3\Sigma^-$ (9)
$a'^3\Sigma^+{}_{0^-}$	17920	2.53	310	$a^3\Sigma^+$ (95), $^1\Sigma^-$ (5)
$^3\Delta_2$	19350	2.52	316	$^3\Delta$ (73), $^1\Delta$ (27)
$^3\Delta_1$	19380	2.53	315	$^3\Delta$ (99)
$^3\Delta_3$	21000	2.53	309	$^3\Delta$ (99)
$^1\Sigma^-{}_{0^-}$	21410	2.52	321	$^1\Sigma^-$ (94), $a^3\Sigma^+$ (5)
$C^3\Sigma^-{}_{0^+}$	21485 (22380)[a]	2.53	319	$^3\Sigma^-$ (98), $b^3\Pi$ (1)
$C'\,^3\Sigma^-{}_1$	21900 (22480)[a]	2.53	319	$^3\Sigma^-$ (89), $a^3\Sigma^+$ (10)
$A^3\Pi_{0^+}$	22268 (22021.3)[a]	2.35	360	$b^3\Pi^-$ (57), $c^3\Sigma^-$ (41)
$^1\Delta_2$	22270	2.54	315	$^1\Delta$ (73), $^3\Delta$ (27)
0^-(III)	22730	2.42	413	$b^3\Pi$ (57), $^1\Sigma^-$ (41)
B1	23370 (23320)[a]	2.42	422	$b^3\Pi$ (83), $c^3\Sigma^-$ (12)
$^3\Pi_2$	24420	2.40	427	$b^3\Pi$ (93)
$D^1\Pi_1$	28023 (28360)[b]	2.42	319	$D^1\Pi$ (96), $b^3\Pi$ (4)
$E^1\Sigma^+{}_{0^+}$	32610	2.59	288	$E^1\Sigma^+$ (98)

[a] Reference 11. [b] Reference 9.

The computed equilibrium bond length of $2^2\Pi$ is 3.10 Å with $\omega_e = 178$ cm^{-1}. The potential energy curve of the $B^2\Sigma^+$ state undergoes an avoided crossing. The fitted r_e and ω_e of this state are 2.44 Å and 195 cm^{-1}, respectively. The estimated transition energy at equilibrium is about 27770 cm^{-1}.

The dissociation energies (D_e) of $X^2\Pi$ and $A^2\Sigma^+$ states of SnS^+ are 2.86 and 2.39 eV, respectively from nine-electron CI calculations. The d-electron correlation increases the dissociation energies by about 0.15 eV.

IV. Spectroscopic Properties of Low-Lying Ω States

A. SnS. All 18 Λ−S states of SnS are included in the spin−orbit coupling. In Figure 3, parts a and b, we have shown the computed potential energy curves of 0^+ and 1 states, respectively. Spectroscopic constants of 16 spin−orbit components are reported in Table 5. The ground-state component ($X^1\Sigma^+{}_{0^+}$) remains unchanged due to the spin−orbit coupling. The energy separation between the 0^- and 1 components of $^3\Sigma^+$ is only 210 cm^{-1}. The computed transition energy of the $a^3\Sigma^+{}_1$−$X^1\Sigma^+{}_{0^+}$ transition is around 17710 cm^{-1}, which is somewhat smaller than $T_e = 18143.9$ cm^{-1} observed for $a1(^3\Sigma^+)$ in the chemiluminescent flame spectrum of SnS.[11] Three components of $^3\Delta$ split in the energy order $^3\Delta_1 \approx {}^3\Delta_2 < {}^3\Delta_3$. The largest splitting is about 1650 cm^{-1}. The components of $^3\Sigma^-$, denoted as $C^3\Sigma^-{}_{0^+}$ and $C'^3\Sigma^-{}_1$, are separated by 400 cm^{-1}. The extended rotational analyses of the perturbed bands observed[11] in the absorption spectrum have made the assignments of the 0^+ and 1 components of $^3\Sigma^-$. The MRDCI-estimated transition energies of both the spin-forbidden transitions, $C^3\Sigma^-{}_{0^+}$−$X^1\Sigma^+{}_{0^+}$ and $C'^3\Sigma^-{}_1$−$X^1\Sigma^+{}_{0^+}$ are smaller than the observed values by 500−900 cm^{-1}. There is a considerable amount of mixing between $^3\Pi_{0^+}$ and $^3\Sigma^-{}_{0^+}$ near the potential minimum of $^3\Pi$. The diabatic curve of the third root of 0^+ is fitted and designated as $A^3\Pi_{0^+}$. The estimated r_e and ω_e of the $A^3\Pi_{0^+}$ component are 2.35 Å and 360 cm^{-1}, respectively. The computed transition energy of the $A^3\Pi_{0^+}$ component agrees well with the observed T_e of 22021.3 cm^{-1}.[11] The $^3\Pi_1$ curve undergoes several avoided crossings (Figure 3b) in the Franck−Condon region. We have fitted this adiabatic curve and denoted the component as B1. The transition energy of the adiabatically fitted curve of B1($^3\Pi$) is found to be 23370 cm^{-1}. Both $A^3\Pi_{0^+}$−$X^1\Sigma^+{}_{0^+}$ and B1−$X^1\Sigma^+{}_{0^+}$ transitions of SnS are analogous to the strongest spin-forbidden systems in CO, namely the Cameron band ($a^3\Pi$−$X^1\Sigma^+$). The $\Omega = 2$ component of $^3\Pi$ also experiences avoided curve crossings with the $^3\Delta_2$ and $^1\Delta_2$ components. The transition energy of $^3\Pi_0{}^-$, estimated by fitting its adiabatic curve, is about 24420 cm^{-1}. However, this component is spectroscopically less

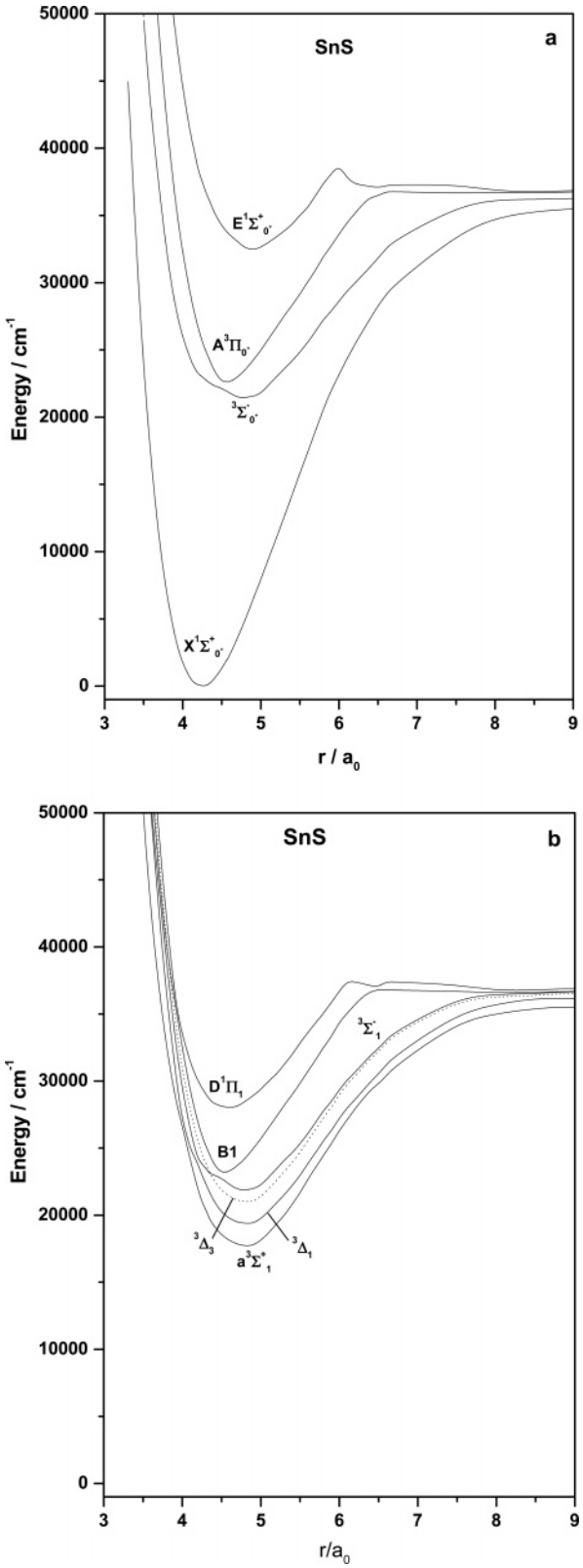

Figure 3. Potential energy curves of some Ω states of SnS for (a) $\Omega = 0^+$ and (b) $\Omega = 1$ and 3.

TABLE 6: Spectroscopic Constants of Ω States of SnS^+

state	T_e/cm^{-1}	r_e/Å	ω_e/cm^{-1}	composition at r_e (% contribution)
$X_1{}^2\Pi_{3/2}$	0	2.41	376	$X^2\Pi$ (98)
$X_2{}^2\Pi_{1/2}$	670	2.42	357	$X^2\Pi$ (98)
$A^2\Sigma^+{}_{1/2}$	4260	2.27	503	$A^2\Sigma^+$ (96), $X^2\Pi$ (3)
$^4\Pi_{3/2}$	16190	2.99	170	$^4\Pi$ (74), $2^2\Pi$ (20)
$^4\Pi_{5/2}$	17800	2.96	188	$^4\Pi$ (99)

important. The $D^1\Pi_1-X^1\Sigma^+{}_{0^+}$ band system of SnS is observed in the absorption spectrum. The computed transition energy of $D^1\Pi_1$ is 28023 cm^{-1} which is in good agreement with the experimental value of 28360 cm^{-1}. The only spin component of the excited Σ^+ state has a potential minimum around 2.59 Å, and it remains almost as pure $E^1\Sigma^+$ in the Franck−Condon region.

B. SnS^+. Parts a and b of Figure 4 show potential energy curves of the low-lying Ω states arising from the spin−orbit interaction among 12 doublet and quartet states which correlate with $Sn^+(^2P_u) + S(^3P_g)$. The computed spin−orbit splitting of the ground state of SnS^+ is about 670 cm^{-1}. Spectroscopic constants of a few low-lying Ω states are given in Table 6. The ground-state component of SnS^+ is $X_1{}^2\Pi_{3/2}$ with almost the same spectroscopic parameters as those of the spin-pure $X^2\Pi$ state. There is an avoided crossing (Figure 4a) between the curves of $X_2{}^2\Pi_{1/2}$ and $A^2\Sigma^+{}_{1/2}$ components around 4.2 a_o. It has decreased ω_e of $X_2{}^2\Pi_{1/2}$ only marginally, while the vibrational frequency of $A^2\Sigma^+{}_{1/2}$ is increased by about 70 cm^{-1}. The transition energy of the $A^2\Sigma^+{}_{1/2}$ component is computed to be 4260 cm^{-1}. The 3/2 and 5/2 components of $^4\Pi$ are also fitted for the estimation of the spectroscopic constants. The energy gap between these two components is as large as 1790 cm^{-1}.

V. Dipole Moments, Transition Moments, and Radiative Lifetimes

A. SnS. Dipole moments (μ_e) of nine low-lying states of SnS at r_e calculated from the MRDCI wave functions without spin−orbit coupling are given in Table 7. Figure 5 shows the dipole moment functions of these states. All the dipole moment curves have minima between 5 and 7 a_o. These curves tend to zero when the bond is elongated to a very large distance. The ground-state dipole moment of SnS is estimated as −3.13 D with the Sn^+S^- polarity. This is very much comparable with the experimental value of −3.18 ± 0.10 D obtained from the Stark-effect measurements on the rotational transitions of SnS. The CCSD(T) calculations of Kellö et al.[19] have estimated a value of −3.05 D. The absolute values of the dipole moments of other excited states are smaller than the ground-state one, but with the same direction of polarity. As expected, the SnS molecule is less polar than the corresponding oxide [μ_e(SnO) = −3.58 D].

Transition dipole moments of five transitions are also plotted in Figure 5 as a function of the bond length. The transition-moment curve for the $E^1\Sigma^+-X^1\Sigma^+$ transition shows a maximum in the Franck−Condon region, while the transition moment of the $D^1\Pi-X^1\Sigma^+$ transition decreases monotonically with the increase in the bond length. The transition-moment curves of $D^1\Pi-{}^1\Delta$, $b^3\Pi-{}^3\Delta$, and $b^3\Pi-a^3\Sigma^+$ are slowly varying and the transition moment values are comparatively small. The nature of these transition moment curves of SnS is strikingly similar to those of SnO. In general, transition moment values of the $E^1\Sigma^+-X^1\Sigma^+$ transition in the equilibrium region are quite large, which makes the transition more probable than others. The computed partial radiative lifetimes for some important transitions at $v' = 0$ are tabulated in Table 8. We have also displayed the effect of the spin−orbit coupling on those transitions in the same table. The lifetime of the $E^1\Sigma^+$ state of SnS is expectedly smaller (∼18 ns) than the other excited states. The $D^1\Pi$ state undergoes three possible transitions such as $D^1\Pi-X^1\Sigma^+$, $D^1\Pi-{}^1\Sigma^-$, and $D^1\Pi-{}^1\Delta$. The transition to the ground state is stronger

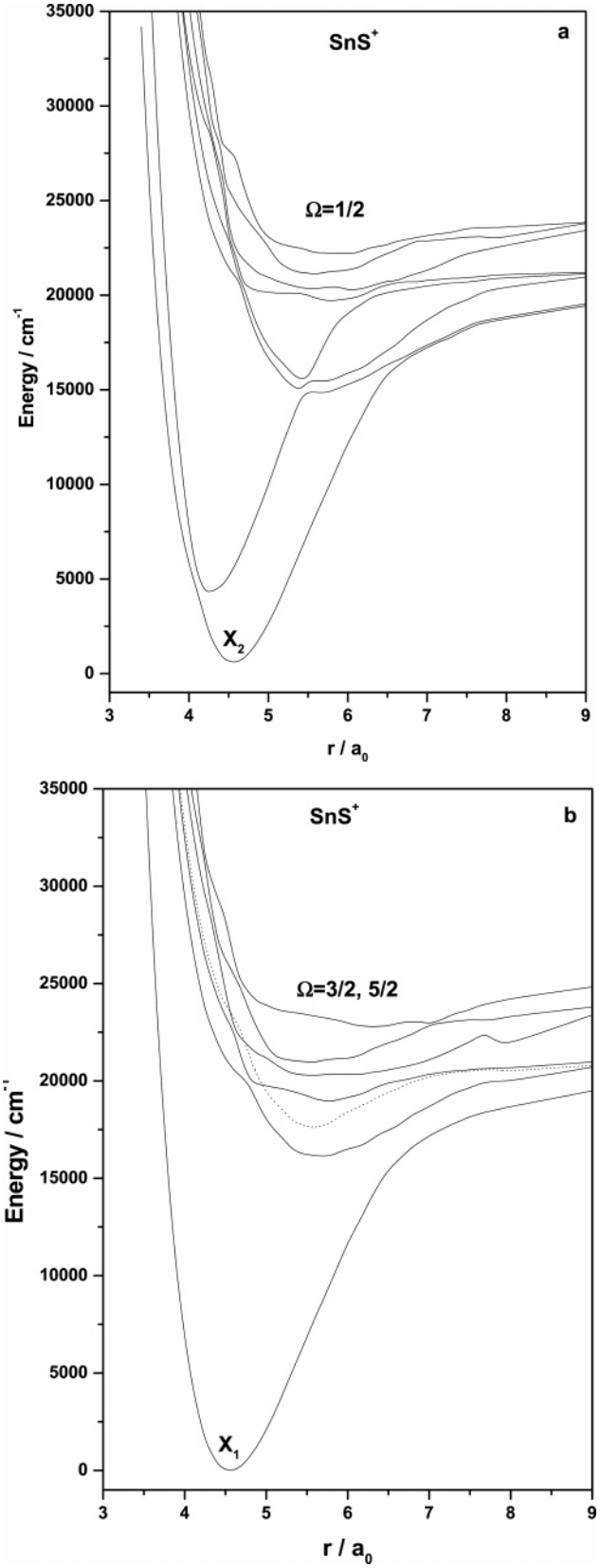

Figure 4. Potential energy curves of some Ω states of SnS^+ for (a) Ω = $^1/_2$ and (b) Ω = $^3/_2$.

TABLE 7: Dipole Moment (μ_e) of Some Low-Lying States of SnS at r_e

state	μ_e/D
$X^1\Sigma^+$	−3.13
	$(-3.18 \pm 0.1)^a$
	$(-3.05)^b$
$a^3\Sigma^+$	−1.06
$^3\Delta$	−0.72
$^1\Sigma^-$	−1.28
$^1\Delta$	−1.18
$c^3\Sigma^-$	−1.12
$b^3\Pi$	−2.30
$D^1\Pi$	−2.29
$E^1\Sigma^+$	−3.04

[a] Reference 16. [b] Reference 19.

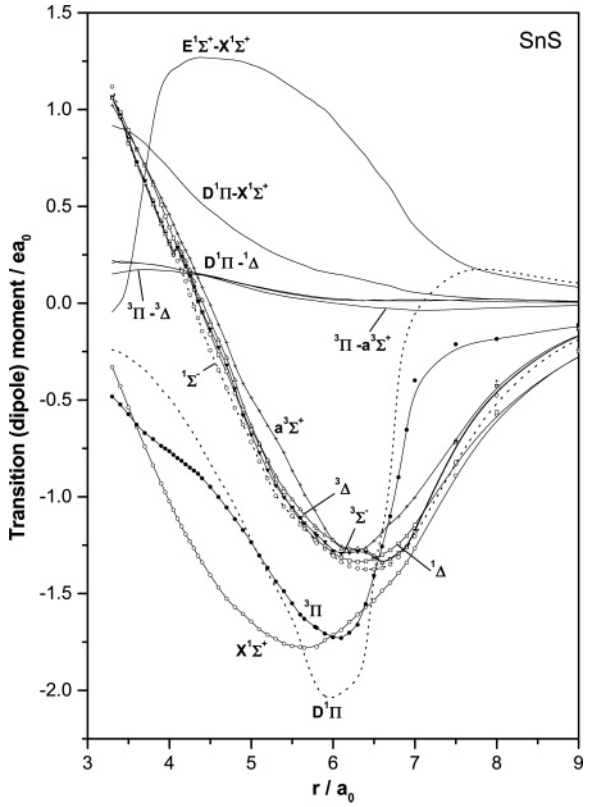

Figure 5. Dipole-moment curves of eight low-lying Λ−S states of SnS and transition-moment curves of five transitions involving Λ states of SnS.

and its partial radiative lifetime is much shorter than the other two. The predicted radiative lifetime of the $D^1\Pi$ state is about 142 ns. Both $b^3\Pi-a^3\Sigma^+$ and $b^3\Pi-{}^3\Delta$ transitions are found to be weak. The energy differences and transition moment values of these two transitions are small. The Franck−Condon factors are also small because of the larger differences in their equilibrium bond lengths. The total radiative lifetime of the $b^3\Pi$ state is about 0.4 ms.

After the inclusion of the spin−orbit coupling, the transition probabilities of $E^1\Sigma^+{}_{0^+}-X^1\Sigma^+{}_{0^+}$ and $D^1\Pi_1-X^1\Sigma^+{}_{0^+}$ transitions do not change much, hence the changes in the radiative lifetimes for these transitions are insignificant. The lifetimes for some spin-forbidden transitions are also listed in Table 8. Both $B1-X^1\Sigma^+{}_{0^+}$ and $A^3\Pi_{0^+}-X^1\Sigma^+{}_{0^+}$ transitions are found to be significant. The partial radiative lifetimes of B1 and $A^3\Pi_{0^+}$ are computed to be around 7 μs at the lowest vibrational level. The present calculations predict that the $C'^3\Sigma^-{}_1-X^1\Sigma^+{}_{0^+}$ transition is weaker ($\tau\sim$ 0.8 ms) than $C^3\Sigma^-{}_{0^+}-X^1\Sigma^+{}_{0^+}$ ($\tau \sim 8$ μs). Transition probabilities for another spin-forbidden transition,

TABLE 8: Radiative Lifetimes (s) for Some Transitions of SnS at $v' = 0$

transition	partial lifetime of the upper state[a]
$E^1\Sigma^+-X^1\Sigma^+$	1.83(−8)
$D^1\Pi-X^1\Sigma^+$	1.42(−7)
$D^1\Pi-{}^1\Sigma^-$	1.26(−4)
$D^1\Pi-{}^1\Delta$	1.55(−4)
$b^3\Pi-a^3\Sigma^+$	3.98(−4)
$b^3\Pi-{}^3\Delta$	4.86(−3)
$E^1\Sigma^+{}_{0^+}-X\ {}^1\Sigma^+{}_{0^+}$	1.74(−8)
$D^1\Pi_1$-$X\ {}^1\Sigma^+{}_{0^+}$	1.40(−7)
$B1-X^1\Sigma^+{}_{0^+}$	7.27(−6)
$A^3\Pi_{0^+}-X^1\Sigma^+{}_{0^+}$	7.07(−6)
$C^3\Sigma^-{}_{0^+}-X\ {}^1\Sigma^+{}_{0^+}$	8.38(−6)
$C'^3\Sigma^-{}_1-X\ {}^1\Sigma^+{}_{0^+}$	7.84(−4)
$a^3\Sigma^+{}_1-X\ {}^1\Sigma^+{}_{0^+}$	1.35(−3)

[a] Numbers in parentheses refer to the power to the base 10.

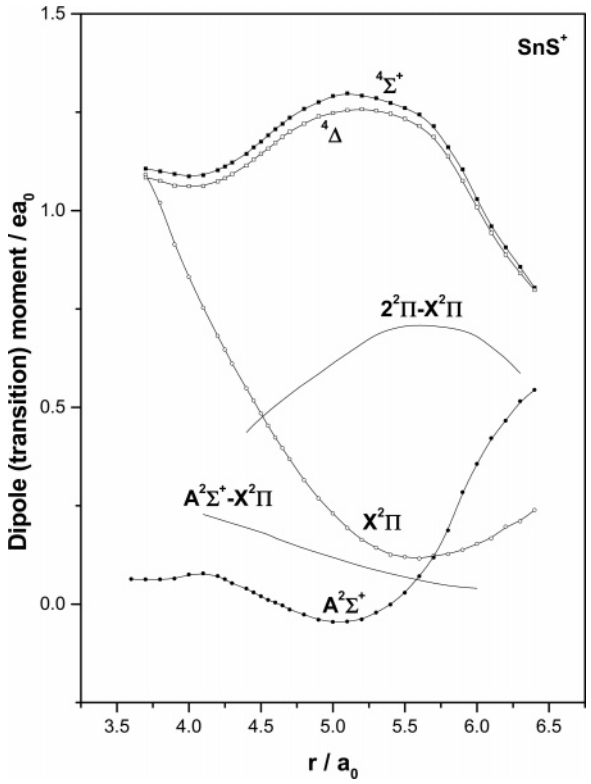

Figure 6. Dipole-moment curves of $X^2\Pi$, $A^2\Sigma^+$, $^4\Sigma^+$, and $^4\Delta$ states, and transition-moment curves of $A^2\Sigma^+-X^2\Pi$ and $2^2\Pi-X^2\Pi$ transitions of SnS^+ (Sn atom is at the origin of the coordinate system).

$a^3\Sigma^+{}_1-X^1\Sigma^+{}_{0^+}$ have been computed here. The partial radiative lifetime for this transition is only 1.35 ms.

B. SnS^+. The dipole moment functions of the $X^2\Pi$, $A^2\Sigma^+$, $^4\Sigma^+$, and $^4\Delta$ states of the ion are shown in Figure 6. The dipole moment values shown in the curves are calculated by keeping Sn at the origin of the Cartesian coordinate system. All the curves are found to be smooth. The doublets of SnS^+ have minima, while the quartets show maxima in their dipole moment curves. The μ_e values, which are calculated by keeping the origin at the center of mass of SnS^+, are listed in Table 9. The ground-state μ_e of SnS^+ is about −1.30 D, while for the first excited state ($A^2\Sigma^+$), it is −2.09 D. The experimental values are not yet known. The knowledge of the dipole moments of the molecular ions may be useful for microwave spectroscopy.

Four low-lying transitions such as $A^2\Sigma^+-X^2\Pi$, $2^2\Pi-X^2\Pi$, $B^2\Sigma^+-X^2\Pi$, and $B^2\Sigma^+-A^2\Sigma^+$ for SnS^+ are reported here. In Figure 6, transition dipole moments of $A^2\Sigma^+-X^2\Pi$ and $2^2\Pi-$

TABLE 9: Dipole Moment (μ_e) of a Few Low-Lying States of SnS^+ at r_e

state	μ_e/D[a]
$X^2\Pi$	−1.30
$A^2\Sigma^+$	−2.09
$2^2\Pi$	1.05
$^4\Pi$	1.61
$^4\Sigma^+$	0.59
$^4\Delta$	0.06

[a] Origin is at the center of mass.

$X^2\Pi$ are plotted as a function of r. The transition moment curve for the A−X transition is monotonically decreasing, while the other one for the $2^2\Pi-X^2\Pi$ transition shows a maximum. Both the curves converge smoothly to zero at large r. The computed transition moments of $B^2\Sigma^+-X^2\Pi$ are larger than those of $B^2\Sigma^+-A^2\Sigma^+$ in the Franck−Condon region. As a result, the partial lifetime of the former transition is shorter than the later one. After the introduction of the spin−orbit coupling, the potential curve of the $B^2\Sigma^+_{1/2}$ component becomes complex in nature due to several avoided curve-crossings. However, both $A^2\Sigma^+_{1/2}-X_1{}^2\Pi_{3/2}$ and $A^2\Sigma^+_{1/2}-X_2{}^2\Pi_{1/2}$ transitions are allowed in the range 3500−4500 cm^{-1}. There are three transition components arising out of the A−X transition. Two components such as $A-X_1$ and $A-X_2$ have perpendicular (⊥) polarizations, while the $A-X_2$ transition component has a parallel (||) polarization. It is predicted here that the $(A-X_2)_\perp$ transition is stronger than $(A-X_2)_{||}$, while the $(A-X_1)_\perp$ transition is the strongest among them. At the lowest vibrational level, the partial radiative lifetime for the $(A-X_1)_\perp$ transition is about 0.7 ms. The transition probabilities of a spin-forbidden transition such as $^4\Pi_{3/2}-X_1{}^2\Pi_{3/2}$ have also been computed, and the radiative lifetime of $^4\Pi_{3/2}$ at $v' = 0$ is about 8 μs.

The vertical ionization energies (VIE) of the ground-state SnS to the ground and some low-lying excited states of SnS^+ are calculated from the differences in the estimated full CI energies. The calculations of both neutral and ionic species have been carried out with the same set of basis functions and configuration-selection threshold. The ground-state equilibrium bond length has been chosen at 4.25 a_o for the calculations of vertical ionization energies. For some of the states such as $X^2\Pi$, $A^2\Sigma^+$, $^4\Sigma^+$, $^4\Pi$, and $^4\Delta$, the effect of d-correlation on the ionization energies has been estimated. From the 19-electron CI calculations, the VIEs of the ground state of SnS to $X^2\Pi$ and $A^2\Sigma^+$ states of SnS^+ are 9.15 and 9.28 eV, respectively, which are comparatively smaller than the values reported for SnO^+.[26] The ionization to the excited $B^2\Sigma^+$ state of SnS^+ requires 12.52 eV energy. Like the oxide ion, the $X_2{}^2\Pi_{1/2}-X_1{}^2\Pi_{3/2}$ transition is extremely difficult to observe because the transition moment values in the Franck−Condon region are only of the order of 0.01 ea_o and the energy difference is less than 1000 cm^{-1}. The calculated radiative lifetime for the X_2-X_1 transition is in the range of 20−30 s only.

VI. Summary

Several low-lying electronic states of SnS and SnS^+ have been computed by the ab initio based MRDCI calculations which include RECP of both Sn and S atoms. The ground state ($X^1\Sigma^+$) of SnS has a closed shell configuration, while the ground state ($X^2\Pi$) of SnS^+ is dominated by an open shell configuration, $\sigma^2\pi^3$. The computed r_e of the ground state of SnS is overestimated by about 0.04 Å, while the calculated ω_e agrees well with the observed value. The inclusion of d electrons in the CI steps does not alter r_e and ω_e of the ground state of SnS significantly. Transition energies (T_e) of the excited bound states are, however, reduced to some extent because of the d-correlation. At the Λ−S level, the $E^1\Sigma^+-X^1\Sigma^+$ and $D^1\Pi-X^1\Sigma^+$ transitions of SnS are stronger. The estimated partial lifetimes of these two transitions are 18 and 142 ns, respectively. The spin−orbit coupling introduces several avoided curve crossings in the potential curves of Ω states of SnS. The spin-forbidden transitions such as $a^3\Sigma^+{}_1-X^1\Sigma^+{}_{0^+}$, $C^3\Sigma^-{}_{0^+}-X^1\Sigma^+{}_{0^+}$, $C'^3\Sigma^-{}_1-X^1\Sigma^+{}_{0^+}$, $A^3\Pi_{0^+}-X^1\Sigma^+{}_{0^+}$, and $B1-X^1\Sigma^+{}_{0^+}$ have been computed and compared with the experimental results. The $E^1\Sigma^+{}_{0^+}-X^1\Sigma^+{}_{0^+}$ transition remains the strongest of all. The ground-state dipole moment (μ_e) of SnS is estimated to be −3.13 D which compares well with the experimentally determined value of −3.18 ± 0.10 D. The ground and first excited states of SnS^+ are $X^2\Pi$ and $A^2\Sigma^+$, respectively. Their spectroscopic constants do not change much due to the d-correlation. On ionization, the ground-state Sn−S bond is enhanced by about 0.16 Å, while the vibrational frequency is reduced by about 100 cm^{-1}. The ground-state dissociation energy of SnS^+ is about 2.86 eV, while that of the neutral species is estimated to be 4.71 eV. The $A^2\Sigma^+$ state of SnS^+ has a shorter bond length and larger vibrational frequency than the ground-state values. Other excited quartets and doublets computed here are weakly bound. The spin−orbit splitting between the two components of $X^2\Pi$ of SnS^+ is found to be around 700 cm^{-1}. Many of the excited 1/2 and 3/2 components of SnS^+ predissociate through various channels. The computed partial lifetimes of the $A-X_1$ and $A-X_2$ transitions with perpendicular polarization are somewhat shorter than that of the $A-X_2$ transition with parallel polarization. The total predicted lifetime of the A state is about 0.4 ms. The X_2-X_1 transition is very weak, and hence difficult to detect experimentally. By keeping the origin at the center of mass, one can predict the dipole moment of the ground state of SnS^+ to be −1.30 D. Finally, the vertical ionization energy of the ground-state SnS to the ground state of its ion is about 9.13 eV.

TABLE 10: Radiative Lifetimes (s) for Some Transitions of SnS^+ at $v' = 0$

transition	partial lifetime of the upper state[a]
$A^2\Sigma^+-X^2\Pi$	6.40(−4)
$2^2\Pi-X^2\Pi$	1.19(−6)
$B^2\Sigma^+-X^2\Pi$	6.04(−7)
$B^2\Sigma^+-A^2\Sigma^+$	4.62(−6)
$A^2\Sigma^+_{1/2}-X_1{}^2\Pi_{3/2}(\perp)$	6.87(−4)
$A^2\Sigma^+_{1/2}-X_2{}^2\Pi_{1/2}(\perp)$	1.13(−3)
$A^2\Sigma^+_{1/2}-X_2{}^2\Pi_{1/2}(\|\|)$	6.29(−3)
$^4\Pi_{3/2}-X_1{}^2\Pi_{3/2}$	8.58(−6)

[a] Numbers in parentheses refer to the power to the base 10.

TABLE 11: Vertical Ionization Energies (eV) of SnS

	calculated IE	
ionic state	without d-electron	with d-electron
$X^2\Pi$	9.13	9.15
$A\ ^2\Sigma^+$	9.41	9.28
$^4\Pi$	12.72	12.58
$2^2\Pi$	13.34	
$^4\Sigma^+$	11.85	11.92
$^4\Delta$	12.21	12.25
$3^2\Pi$	13.45	
$B\ ^2\Sigma^+$	12.52	

Acknowledgment. We thank Prof. Dr. Robert J. Buenker, Wuppertal, Germany, for making available the CI codes. The financial support from CSIR, Govt. of India under the scheme 01(1759)/02/EMR-II is gratefully acknowledged.

References and Notes

(1) Butkow, K.; Tschassowenny, W. *Z. Phys.* **1934**, *90*, 53.
(2) Rochester, G. D. *Proc. R. Soc. London* **1935**, *A150*, 668.
(3) Shawhan, E. N. *Phys. Rev.* **1935**, *48*, 521.
(4) Shawhan, E. N. *Phys. Rev.* **1936**, *49*, 810.
(5) Douglas, A. E.; Howe, L. L.; Morton, J. R. *J. Mol. Spectrosc.* **1961**, *7*, 161.
(6) Barrow, R. F.; Drummond, G.; Rowlinson, H. C. *Proc. Phys. Soc. (London)* **1953**, *A66*, 885.
(7) Colin, R.; Drowart, J. *J. Chem. Phys.* **1962**, *37*, 1120.
(8) Yamdagni, R.; Joshi, M. M. *Ind. J. Phys.* **1966**, *40*, 495.
(9) Smith, J. J.; Meyer, B. *J. Mol. Spectrosc.* **1968**, *27*, 304.
(10) Marino, C. P.; Guerin, J. D.; Nixon, E. R. *J. Mol. Spectrosc.* **1974**, *51*, 160.
(11) Greenwood, D. J.; Linton, C.; Barrow, R. F. *J. Mol. Spectrosc.* **1981**, *89*, 134.
(12) Balasubramanian, K.; Pitzer, K. S. *Chem. Phys. Lett.* **1983**, *100*, 273.
(13) Balasubramanian, K. *Chem. Phys. Lett.* **1987**, *139*, 262.
(14) Nair, K. P. R,; Singh, R. B.; Rai, D. K. *J. Chem. Phys.* **1965**, *43*, 3570.
(15) Giri, D.; Buenker, R. J.; Das, K. K. *J. Phys. Chem.* **2002**, *A106*, 8790.
(16) Hoeft, J.; Lovas, F. J.; Tiemann, E.; Tischer, R.; Törring, T. *Z. Naturforsch. A* **1969**, *24*, 1222.
(17) Hoeft, J.; Lovas, F. J.; Tiemann, E.; Törring, T. *J. Chem. Phys.* **1970**, *53*, 2736.
(18) Narasimha Murty, A.; Curl, Jr. R. F. *J. Mol. Spectrosc.* **1969**, *30*, 102.
(19) Kellö, V.; Sadlej, A. J.; Fægri, Jr. K. *J. Chem. Phys.* **1998**, *108*, 2056.
(20) Lefebvre, I.; Szymanski, M. A.; Olivier-Fourcade, J.; Jumas, J. C. *Phys. Rev. B* **1998**, *58*, 1896.
(21) Colbourn, E. A.; Dyke, J. M.; Lee, E. P. F.; Morris, A.; Trickle, I. R. *Mol. Phys.* **1978**, *35*, 873.
(22) Colbourn, E. A.; Dyke, J. M.; Fackerell, A.; Morris, A.; Trickle, I. R. *J. Chem. Soc., Faraday Trans. 2* **1977**, *73*, 2278.
(23) White, M. G.; Rosenberg, R. A.; Lee, S. T.; Shirley, D. A. *J. Electron Spectrosc. Relat. Phenom.* **1979**, *17*, 323.
(24) Dyke, J. M.; Morris, A.; Ridha, A. M. A.; Snijders, J. G. *Chem. Phys.* **1982**, *67*, 245.
(25) Bredohl, H.; Breton, J.; Dubois, I.; Esteva, J. M.; Macauttercot, D.; Remy, F. *J. Mol. Spectrosc.* **1998**, *187*, 163.
(26) Giri, D.; Das, K. K. *Chem. Phys. Lett.* **2003**, *368*, 465.
(27) John, L. A.; Christiansen, P. A.; Ross, R. B.; Atashroo, T.; Ermler, W. C. *J. Chem. Phys.* **1987**, *87*, 2812.
(28) Pacios, L. F.; Christiansen, P. A. *J. Chem. Phys.* **1985**, *82*, 2664.
(29) Alekseyev, A. B.; Liebermann, H.-P.; Buenker, R. J.; Hirsch, G. *Mol. Phys.* **1996**, *88*, 591.
(30) Lingott, R. M.; Liebermann, H.-P.; Alekseyev, A. B.; Buenker, R. J. *J. Chem. Phys.* **1999**, *110*, 11294.
(31) Buenker, R. J.; Peyerimhoff, S. D. *Theor. Chim. Acta* **1974**, *35*, 33.
(32) Buenker, R. J.; Peyerimhoff, S. D. *Theor. Chim. Acta* **1975**, *39*, 217.
(33) Buenker, R. J.; Peyerimhoff, S. D.; Butscher, W. *Mol. Phys.* **1978**, *35*, 771.
(34) Buenker, R. J. *Int. J. Quantum Chem.* **1986**, *29*, 435.
(35) Buenker, R. J. In *Proceedings of the Workshop on Quantum Chemistry and Molecular Physics*; Burton, P., Ed.; University Wollongong: Wollongong, Australia; 1980.
(36) Buenker, R. J. In *Studies in Physical and Theoretical Chemistry*; Carbó, R., Ed.; Elsevier: Amsterdam, 1981; Vol. 21 (Current Aspects of Quantum Chemistry).
(37) Buenker, R. J.; Phillips, R. A. *J. Mol. Struct. (THEOCHEM)* **1985**, *123*, 291.
(38) Davidson, E. R. In *The World of Quantum Chemistry*; Daudel, R., Pullman, B., Ed.; Reidel: Dordrecht, The Netherlands, 1974.
(39) Moore, C. E. *Atomic Energy Levels*; National Bureau of Standards: Washington, DC; 1971; Vol. 3.